

UDK 621.315.592

Features in the behavior of temperature dependences of magnetic susceptibility of crystals of $\text{Bi}_2\text{Te}_3\text{—Sb}_2\text{Te}_3$ solid solutions containing from 25 to 70 percent antimony telluride

© N.P. Stepanov¹, M.S. Ivanov²

¹ Trans-Baikal State University,
672036 Chita, Russia

² Trans-Baikal Institute of Railway Transport,
672040 Chita, Russia

E-mail: np-stepanov@mail.ru

Received October 23, 2022

Revised November 17, 2022

Accepted December 22, 2022

Temperature dependences of the magnetic susceptibility of *p*-type crystals of $\text{Bi}_2\text{Te}_3\text{—Sb}_2\text{Te}_3$ solid solutions containing from 25 to 70 mol percent antimony telluride were examined in the range from 2 to 400 K. A correlation was found between the features observed in the behavior of temperature dependences of the magnetic susceptibility of crystals containing 60 and 70 mol percent Sb_2Te_3 and the ratio of the plasmon energy to the energy of the gap between the chemical potential level and the heavy hole subband. An assumption is formulated that in the case of convergence of these energies, the increasing electron–plasmon interaction affects the electron system state and, consequently, the magnitude of magnetic susceptibility.

Keywords: bismuth and antimony tellurides, magnetic susceptibility, plasmon, interband transitions, electron–plasmon interaction.

DOI: 10.21883/SC.2022.12.55145.4243

1. Introduction

Since Bi_2Te_3 crystals are used as thermoelectric materials, their band structure, which is distinguished by a complex valence band with two non-equivalent extrema [1], has been studied extensively. A complex structure of the conduction band was also noted in several studies [2–4]. The arrangement of electron shells of $\text{Bi}_2\text{Te}_3\text{—Sb}_2\text{Te}_3$ crystals is similar to the one of Bi_2Te_3 . This is the reason why their band structures are also close; the difference is that the bandgap width changes in transition to Sb_2Te_3 [5], and the heavy hole subband shifts deeper into the valence band [6]. As the concentration of Sb_2Te_3 in solid solution $\text{Bi}_2\text{Te}_3\text{—Sb}_2\text{Te}_3$ grows, the density of light holes also increases to $8 \cdot 10^{19} \text{ cm}^{-3}$ [7]. This increase in density of light holes is accompanied by a shift of the chemical potential level deeper into the valence band [8,9]. The energy gap between the heavy hole subband and the chemical potential level also changes in the process. The magnitude of this gap in *p*-type $\text{Bi}_2\text{Te}_3\text{—Sb}_2\text{Te}_3$ crystals plays an essential role in temperature variation of certain parameters affecting their thermoelectric efficiency and response to electric and magnetic fields, since it specifies the intensity of thermal transitions of carriers between the valence band extrema and, consequently, defines the density of light mobile holes. The considered materials feature an anomalous temperature behavior of the Hall coefficient [1], and the density of light holes in them was found to decrease after doping with impurities that should presumably have an acceptor effect [10]. Therefore, it is of some interest to investigate the

trends of variation of their electron system with composition of the solid solution and temperature. In the present study, this was done by examining the temperature dependences of the magnetic susceptibility of $\text{Bi}_2\text{Te}_3\text{—Sb}_2\text{Te}_3$ crystals. Note that the magnetic susceptibility is an equilibrium thermodynamic parameter and, in contrast to, e.g., specific electric and thermal conductivities, which are commonly examined (alongside with the thermoelectric coefficient) in thermoelectric materials, is independent of the intensity of relaxation processes; however, it is determined in large part by the density of free carriers. Thus, magnetic susceptibility studies provide an opportunity to analyze in more detail the changes in the electron system state of a material induced by variations of composition of the solid solution and temperature. In view of this, the present study is aimed at investigating the trends of variation of temperature dependences of the magnetic susceptibility on the ratio of components Bi_2Te_3 and Sb_2Te_3 in solid solution $\text{Bi}_2\text{Te}_3\text{—Sb}_2\text{Te}_3$ and analyzing them with account for the temperature variation of other physical quantities characterizing the state of the electron system of a crystal.

2. Crystals, samples, experimental procedure

Single crystals of $\text{Bi}_2\text{Te}_3\text{—Sb}_2\text{Te}_3$ solid solutions containing 25, 50, 60, and 70 mol% Sb_2Te_3 and grown by the Czochralski method at the Baikov Institute of Metallurgy and Materials Science were examined.

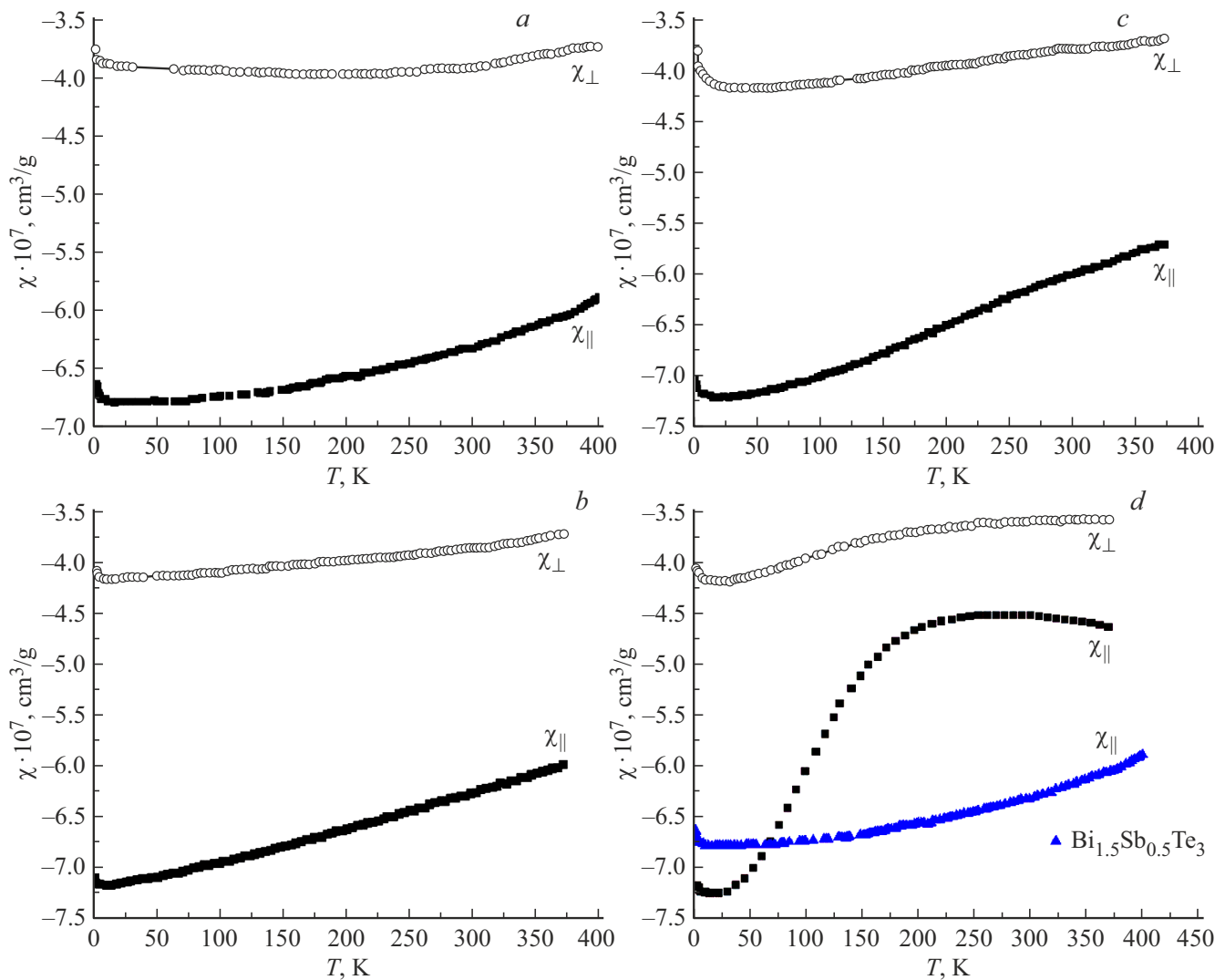


Figure 1. *a* — Dependence of magnetic susceptibility χ_{\parallel} and χ_{\perp} on the temperature of crystals of solid solution $\text{Bi}_{1.5}\text{Sb}_{0.5}\text{Te}_3$ (25 mol% Sb_2Te_3); *b* — BiSbTe_3 (50 mol% Sb_2Te_3); *c* — $\text{Bi}_{0.4}\text{Sb}_{0.2}\text{Te}_3$ (60 mol% Sb_2Te_3); *d* — $\text{Bi}_{0.6}\text{Sb}_{1.4}\text{Te}_3$ (70 mol% Sb_2Te_3). The susceptibility was measured in a field of 14 kOe.

The results of measurements of the magnetic susceptibility at temperatures ranging from 2 to 400 K performed in magnetic fields up to 30 kOe using a superconducting quantum interference device (Magnetic Property Measurement System (MPMS MultiVu) SQUID magnetometer produced by Quantum Design) are reported in the present study. The measurements were performed for two different orientations of magnetic field vector H relative to C_3 ($H \parallel C_3$ and $H \perp C_3$). The value of χ_{\parallel} was determined at $H \parallel C_3$, while χ_{\perp} corresponds to the $H \perp C_3$ orientation. A complete description of samples and the experimental procedure and equipment is provided in [11].

3. Discussion of experimental results

The results of examination of the magnetic susceptibility of $\text{Bi}_{1.5}\text{Sb}_{0.5}\text{Te}_3$ (25 mol% Sb_2Te_3), BiSbTe_3

(50 mol% Sb_2Te_3), $\text{Bi}_{0.4}\text{Sb}_{0.2}\text{Te}_3$ (60 mol% Sb_2Te_3), and $\text{Bi}_{0.6}\text{Sb}_{1.4}\text{Te}_3$ (70 mol% Sb_2Te_3) samples in the temperature range of 2–400 K are presented in Fig. 1. For improved readability, the Sb_2Te_3 content of solid solution $\text{Bi}_2\text{Te}_3\text{—Sb}_2\text{Te}_3$ (in mol%) is indicated in what follows instead of the chemical formula of the sample.

It should be noted that dependences of the magnetic moment on the field strength were found in preliminary studies to remain linear up to 30 kOe in all samples. This dependence for the crystal containing 10 mol% Sb_2Te_3 is shown in Fig. 2 and indicates that the value of magnetic susceptibility is independent of the magnetic field strength. The magnetization behavior in all the other studied samples was similar.

It can be seen from Fig. 1 that all samples feature a diamagnetic response with its magnitude being dependent on the orientation of H relative to axis C_3 , temperature, and the Sb_2Te_3 content of solid solution $\text{Bi}_2\text{Te}_3\text{—Sb}_2\text{Te}_3$. Since

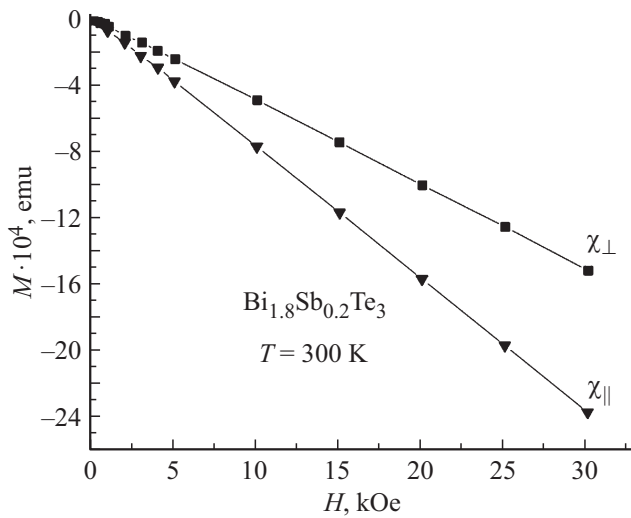


Figure 2. Dependence of magnetization M of the crystal sample containing 10 mol% Sb_2Te_3 on field strength H measured at a temperature 300 K.

the variations of $\chi_{\parallel}(T)$ with increasing Sb_2Te_3 concentration are more pronounced, the initial analysis of experimental data was focused on the behavior of $\chi_{\parallel}(T)$. It is fair to say that a change in the nature of $\chi_{\parallel}(T)$ dependences is observed in Fig. 1. To illustrate this change more clearly, the χ_{\parallel} curve for the crystal with 25 mol% Sb_2Te_3 was plotted in Fig. 1, *d*. Specifically, the $\chi_{\parallel}(T)$ curve for the crystal containing 25 mol% Sb_2Te_3 is „concave“ in the temperature interval from 50 to 400 K, but a transition to the „convex“ shape is observed when the Sb_2Te_3 concentration increases. The shape of temperature dependences of the first derivative of magnetic susceptibility (see Fig. 3) also changes considerably in the process. Indeed, it follows from Figs. 1, *a* and 3 that the first derivative of magnetic susceptibility $d\chi/dT$ increases monotonically with temperature in the crystal containing 25 mol% Sb_2Te_3 and that the slope of dependence $\chi(T)$ increases continuously in the interval from 100 to 400 K. In the crystal containing 50 mol% Sb_2Te_3 (see Fig. 1, *b*), $d\chi/dT$ remains almost constant, thus indicating an emerging trend toward variation of the shape of the temperature dependence. This trend becomes more pronounced in the crystal containing 60 mol% Sb_2Te_3 (Fig. 1, *c*): its $\chi_{\parallel}(T)$ dependences reveal a reduction in $d\chi/dT$ at $T > 250$ K, which is evident in Fig. 3. The crystal containing 70 mol% Sb_2Te_3 (Fig. 1, *d*) features a well-pronounced $d\chi/dT$ maximum at a temperature of 100 K (see Fig. 3), which is followed by the decay of $d\chi/dT$ to zero at $T \approx 250$ K, a change in the sign of the first derivative, and the growth of diamagnetic susceptibility of the crystal.

It should be emphasized that the shape change of temperature dependences of the magnetic susceptibility occurring as the Sb_2Te_3 content increases to 60 mol% is, as follows from Fig. 1, accompanied by the growth of diamagnetic susceptibility at a temperature of 15 K. In view of increases in the density of light holes and the

specific electric conductivity [7], this is indicative of a diamagnetic nature of the response. However, a certain process, the results of which were characterized above, induces a reverse effect at a temperature of 250 K: the diamagnetic response of a crystal becomes weaker as the Sb_2Te_3 content increases (see Fig. 4). It follows from Fig. 4 that the suppression of diamagnetism is the most pronounced in the crystal containing 70 mol% Sb_2Te_3 . It should also be noted that the discussed process is activated in this crystal at low temperatures; the rate of variation of the magnetic susceptibility reaches its maximum at 100 K and decreases smoothly at higher temperatures (see Fig. 3), but the process continues and produces the greatest effect at 250 K. It is reasonable to assume in this context that the process activation temperature corresponds to the maximum of the first derivative of magnetic susceptibility. It follows from Fig. 3 that this temperature is 275 and 100 K for crystals containing 60 and 70 mol% Sb_2Te_3 , respectively. At the same time, the data presented in Figs. 1, *c, d* and 3 suggest that the intensity of the considered process in the crystal with 60 mol% Sb_2Te_3 is lower (and the activation temperature is higher) than in the crystal containing 70 mol% Sb_2Te_3 . This is the reason why thermal diffusion conceals its resonance properties, which are manifested clearly in the temperature dependences of the magnetic susceptibility of the crystal containing 70 mol% Sb_2Te_3 . It is conceivable that the indicated process also affects the crystal containing 50 mol% Sb_2Te_3 (Fig. 1, *b*) and deforms the $\chi(T)$ curve, which differs in shape from the „concave“ $\chi(T)$ curve of the crystal containing 25 mol% Sb_2Te_3 . Thus, the indicated features of temperature dependences of the magnetic susceptibility of Bi_2Te_3 – Sb_2Te_3 crystals reveal the influence of a process of an unknown nature. As the Sb_2Te_3 percentage content grows, the activation temperature of this process decreases, while the process intensity increases.

In order to determine the nature of this process, we examine the response of a semiconductor crystal to an

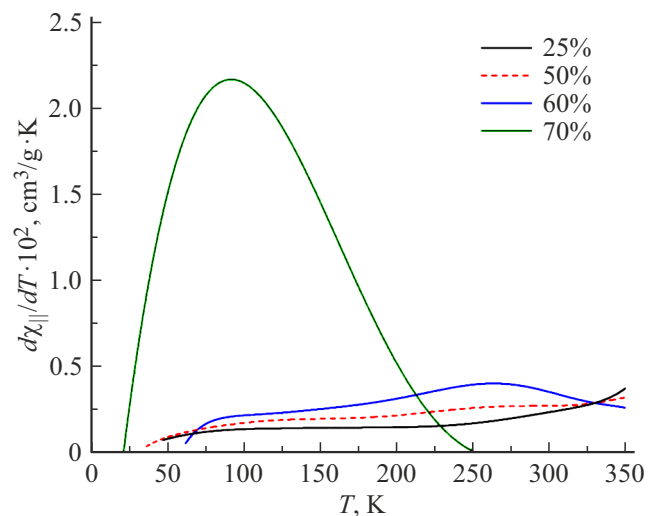


Figure 3. Temperature dependences $d\chi_{\parallel}/dT$ for crystals with 25, 50, 60, and 70 mol% Sb_2Te_3 in the composition of solid solution Bi_2Te_3 – Sb_2Te_3 .

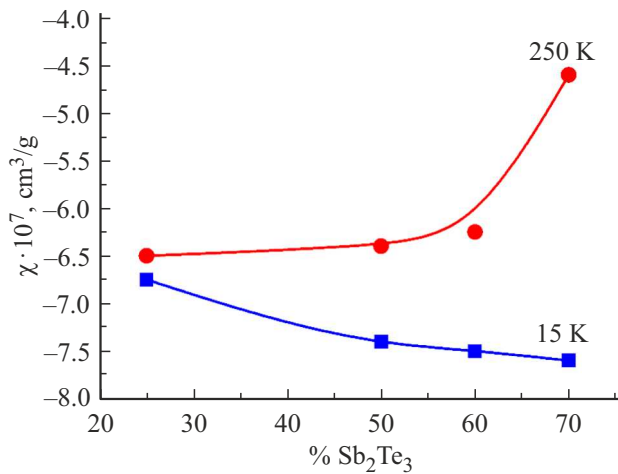


Figure 4. Variation of the magnetic susceptibility of the studied Bi₂Te₃–Sb₂Te₃ crystals with the Sb₂Te₃ content (mol%) at temperatures of 15 and 250 K.

external magnetic field. It is known [12,13] that net magnetic susceptibility χ of crystals may be presented as a sum of contributions of lattice defects χ^d , the ion core χ^G , and free carriers χ^{eh} :

$$\chi = \chi^d + \chi^G + \chi^{eh}. \quad (1)$$

It was established in [13] that the χ^d contribution in Bi₂Te₃ crystals is negligible. The χ^G and χ^{eh} contributions may be comparable in magnitude. The density of free carriers in semiconductors normally decreases considerably at low temperatures, and the experimental values of magnetic susceptibility are, as was noted by Busch and Mooser [14], then defined exclusively by χ^G . However, the violation of stoichiometry and impurities with a low ionization potential in Bi₂Te₃ crystals maintain the density of free carriers at the level of $\sim 1 \cdot 10^{19} \text{ cm}^{-3}$ even at very low temperatures. This precludes one from using the Busch–Mooser approach to determine the value of χ^G . It follows from Fig. 1 that the magnetic susceptibility is anisotropic at $T = 2 \text{ K}$, which is attributable to the anisotropy of effective masses of free carriers (even if the magnetic response of the ion core is isotropic). In view of this, it appears reasonable to estimate the value of χ^G first. Let us consider the approach to analysis of the magnetic susceptibility data for Bi₂Te₃ and Sb₂Te₃ crystals that was used in [13]. Relying on the assumption that the magnetic susceptibility in semiconductor crystals with a certain bond ionicity is governed at low temperatures by the contribution of the ion core, the authors of [13] calculated the molar susceptibility of Bi₂Te₃ in accordance with the classical Langevin formula. This approach provided a fine agreement between number Z of electrons in Bi₂Te₃, Sb₂Te₃ molecules and their molar susceptibility. Specifically, Bi₂Te₃ has $Z = 322$ and molar susceptibility $\chi_{\text{mol}} = -322 \cdot 10^{-6} \text{ cm}^3$, which corresponds to specific susceptibility $\chi = -0.4 \cdot 10^{-6} \text{ cm}^3/\text{g}$ and agrees closely with the results of experimental studies for polycrystals [13].

The susceptibility of the ion core of Bi₂Te₃–Sb₂Te₃ crystals was examined in [15]. A new method for determination of the magnetic susceptibility of the ion core in anisotropic materials was proposed. Specifically, relying on the assumption of χ^G isotropy and taking the known anisotropy of effective masses of free carriers in Bi₂Te₃–Sb₂Te₃ crystals [1] into account, the authors of [15] used the Pauli and Landau–Peierls approaches to characterize the magnetic susceptibility of free carriers and managed to obtain χ_{\parallel} and χ_{\perp} values that are consistent with the experimentally observed magnetic susceptibility (on condition that $\chi^G = -0.35 \cdot 10^{-6} \text{ cm}^3/\text{g}$). To conclude the analysis of data on the magnetic susceptibility of the ion core of Bi₂Te₃–Sb₂Te₃ crystals, we note that this susceptibility was also estimated in [16] at $\chi^G = -0.33 \cdot 10^{-6} \text{ cm}^3/\text{g}$, which is fairly close to the value obtained in [15]. It follows from the presented data that the magnetic susceptibility of the ion core of Bi₂Te₃–Sb₂Te₃ crystals is isotropic in nature and cannot vary significantly with temperature. Therefore, the anisotropy of magnetic susceptibility and its temperature dependence, which are observed in Fig. 1, are attributable to free carriers (χ^{eh}).

It is known that free-carrier contribution $\chi^{eh} = \chi^P + \chi^{LP}$ is, in turn, divisible into paramagnetic Pauli χ^P and diamagnetic Landau–Peierls χ^{LP} contributions. It was demonstrated in [17] that the values of χ_{\perp}^{eh} and χ_{\parallel}^{eh} in anisotropic semiconductor crystals should be calculated with account for the anisotropy of effective carrier masses in accordance with the following expressions:

$$\chi_{\perp}^{eh} = \frac{3^{1/3}}{\pi^{4/3}} \cdot \frac{\mu_B^2 m_{\perp}^* n^{1/3}}{\hbar^2} \left(1 - \frac{1}{3} \left(\frac{m_0^2}{m_{\perp}^* m_{\parallel}^*} \right) \right), \quad (2)$$

$$\chi_{\parallel}^{eh} = \frac{3^{1/3}}{\pi^{4/3}} \cdot \frac{\mu_B^2 m_{\parallel}^* n^{1/3}}{\hbar^2} \left(1 - \frac{1}{3} \left(\frac{m_0}{m_{\perp}^*} \right)^2 \right). \quad (3)$$

Expressions (2) and (3) feature effective susceptibility masses of free carriers $m_{\perp}^* = 0.09m_0$, $m_{\parallel}^* = 0.22m_0$, which were calculated within the six-ellipsoid Drabble–Wolfe model [1]. Since m_{\perp}^* and m_{\parallel}^* are significantly smaller than $0.577m_0$, it can be shown by direct calculations that χ_{\perp}^{eh} and χ_{\parallel}^{eh} assume negative values. The results of analysis of an experimental data set performed in [11] also reinforce the conclusion that the response of free carriers in Bi₂Te₃–Sb₂Te₃ crystals is diamagnetic in nature.

It follows from Fig. 1 that the diamagnetic susceptibility of all samples decreases at higher temperatures. Since the magnetic susceptibility of the ion core is independent of temperature, it is fair to state that the observed temperature dependence of the magnetic susceptibility is attributable to free carriers and is induced by a reduction in the density of light diamagnetic holes. Therefore, the influence of the discovered process, which accelerates the reduction of diamagnetic susceptibility within a certain temperature interval and varies in intensity depending on the Sb₂Te₃ content of solid solution Bi₂Te₃–Sb₂Te₃, may also be attributed to a reduction in the density of light holes.

Let us examine the probable causes of reduction of the density of light diamagnetic holes in Bi_2Te_3 – Sb_2Te_3 crystals. It is known that the process of transition of carriers from the heavy hole subband to the subband of light holes in the considered materials intensifies at higher temperatures, thus reducing the density of light holes [1]. This temperature increase in the density of heavy holes at the expense of light ones is the most probable reason behind an anomalous enhancement of the Hall coefficient that is observed not only in Bi_2Te_3 – Sb_2Te_3 crystals, but also, e.g., in PbTe crystals, which too have a complex structure of the valence band [18]. Specifically, an anomalous behavior of the Hall coefficient is observed at temperatures up to 300 K in Bi_2Te_3 crystals and up to 600 K in Sb_2Te_3 crystals. The reduction in diamagnetic susceptibility with an increase in temperature to 400 K, which is seen in Fig. 1 for all the studied crystals, may then also be attributed to the process of transition of holes between non-equivalent extrema of the valence band as a result of thermal excitation of electrons from the heavy hole subband to the chemical potential level located in the light hole subband. Since the probability of these transitions increases exponentially with temperature, an accelerated reduction of the magnetic susceptibility with increasing temperature should be observed. The $\chi(T)$ curve of the crystal containing 25 mol% Sb_2Te_3 agrees, to a certain extent, with this prediction. However, the above-discussed specifics of temperature dependences of the magnetic susceptibility of crystals containing 50, 60, and 70 mol% Sb_2Te_3 suggest that a certain process accelerates the reduction of the density of light diamagnetic holes within a specific temperature interval. This influence, which becomes more pronounced within a specific temperature interval, is complementary to the process of direct thermal transition of holes and differs from it in having a resonance nature.

In establishing the nature of this process, we place an emphasis on the fact that the transition of holes is induced by the transfer of electrons from the heavy hole subband to the chemical potential level located in the light hole subband. Energy ΔE of this transition in Bi_2Te_3 varies within the range from 20 to 30 meV. Specifically, it was proposed in [19] that the obtained experimental data may be interpreted under the assumed presence of an additional subband with a higher effective mass and low mobility located in the valence band of Bi_2Te_3 crystals 20 meV below the upper subband, which defines the thermal width of the bandgap. The presence of a heavy hole subband in Sb_2Te_3 was discussed in [6] in analysis of dependences of the thermal emf on the specific electric conductivity. It turned out that the results of experiments could be interpreted correctly only with the assumed contribution from a heavy hole subband located 230 meV below the light hole subband at 300 K. Since Bi_2Te_3 – Sb_2Te_3 have a similar crystal structure, it is reasonable to expect that their energy band structure is also similar [1]. Therefore, all the studied crystals should have a heavy hole subband, and energy gap ΔE increases from 20 meV in Bi_2Te_3 to ~ 230 meV in Sb_2Te_3 .

The variation of ΔE affect probability V of electron transfer, which decreases with increasing ΔE and grows with temperature as $V \approx e^{-\frac{\Delta E}{kT}}$. In order to gain an insight into the nature of the process accelerating the reduction of density of light diamagnetic holes and thus affecting the temperature dependences of magnetic susceptibility, one needs to examine different ways to raise the probability of the indicated transition. For example, it can be increased at a certain temperature by electromagnetic radiation quanta with an energy of ΔE (in the absorption layer only). In bulk samples that are not subjected to external electromagnetic irradiation, the acceleration of transition of holes is likely attributable to a certain elementary excitation of a crystal with an energy comparable to ΔE . It is known that solids support various elementary excitations of electron and ion subsystems. Notably, plasmons belong to this class of excitations, which also includes phonons, interband transitions, excitons, etc. The data provided below explain why we should focus exactly on this type of excitation of the electron system in the studied materials.

A plasmon is a quantum of longitudinal oscillations of the charge density of free carriers relative to the ion core. Free carrier plasma is found in metals, semimetals, and semiconductors [20]. The current rapid progress in plasmonics [21,22], the development of hardware components for plasmonic integrated circuits [23], and studies of the behavior of plasmons in low-dimensional systems [24,25] make the research into surface and bulk plasmons highly topical. In contrast to metals with plasmon energies E_p exceeding 10 eV, semiconductors feature plasmons with E_p values that may be comparable to the energy of thermal oscillations of the ion core, and plasmons in these materials may be excited thermally [26]. Thus, it is conceivable that plasma also affects the physical properties of the studied crystals. This influence should be most pronounced when the plasmon energy approaches the bandgap width, which characterizes the covalent bond-breaking energy. The electron–plasmon interaction should be enhanced in this case, since its intensity is maximized when the plasmon energy becomes equal to the interband transition energy [27]. It was demonstrated in a number of studies that both plasmons and phonons may be involved in generation and recombination of electron–hole pairs under these conditions [28,29]. Therefore, a fraction of thermal energy will be concentrated in plasma oscillations of free carriers relative to the ion core (i.e., plasmons), and a part of this energy may be spent on generation of electron–hole pairs. Thus, plasmon–phonon polaritons are a potential influencing factor that induces changes in the shape of temperature dependences of the magnetic susceptibility in Fig. 1 that are indicative of the influence of a certain process.

It should be noted in this context that Bi_2Te_3 – Sb_2Te_3 crystals are distinct in having comparable values of plasmon energy E_p and energy gap ΔE between non-equivalent extrema of the valence band. The plasmon energy is then not much higher than the energy of thermal oscillations. Specifically, the minimum values of the plasmon

energy in $\text{Bi}_2\text{Te}_3\text{--Sb}_2\text{Te}_3$ crystals are $\sim 25\text{--}30\text{ meV}$ [30]. Therefore, collective plasma oscillations of free carriers in the considered materials may emerge under the influence of thermal lattice oscillations. The presence of thermal plasmons with energies close to ΔE may affect the state of the electron system and induce the above-described features of temperature dependences of the magnetic susceptibility.

Let us examine the experimental data validating this hypothesis. First off, it should explain the above-discussed relation between the temperature corresponding to the maximum of intensity of the process inducing changes in the shape of temperature dependences of the magnetic susceptibility in Fig. 1 and the percentage content of antimony telluride. It is instructive in this context to examine the variation of the plasmon energy with temperature and composition of the $\text{Bi}_2\text{Te}_3\text{--Sb}_2\text{Te}_3$ solid solution. Specifically, the plasmon energy increases with decreasing temperature in all $\text{Bi}_2\text{Te}_3\text{--Sb}_2\text{Te}_3$ crystals due to an increase in the density of light holes, which is induced by a reduction in the intensity of transition of electrons from the heavy hole subband to the chemical potential level. Since this intensity is weak at low temperatures, the density of light holes and the plasmon energy are higher than the corresponding values at high temperatures. For example, the plasmon energy in *p*-type Bi_2Te_3 varies from 40 meV at 300 K to 50 meV at 78 K [30]. Figure 4 from [31], which presents the temperature dependences of reflectance spectra of the crystal containing 60 mol% Sb_2Te_3 , reveals an increase in the frequency of the plasma reflection minimum (and consequently, the plasmon energy) at lower temperatures. The plasmon energy in this crystal increases by $\sim 20\text{ meV}$ as the temperature decreases from 290 to 79 K. It is also important to note that energy ΔE of the electron transition from the heavy hole subband to the chemical potential level, which is located in the light hole subband, decreases at lower temperatures, since the chemical potential level shifts deeper into the valence band. Figure 2 from [31] also reveals a reduction in the frequency of the diffuse reflectance maximum in the spectral region of 2000 cm^{-1} at higher temperatures. This indicates that the chemical potential level in the crystal containing 60 mol% Sb_2Te_3 shifts to the top of the valence band at higher temperatures, thus inducing an increase in ΔE . The repositioning of the chemical potential level and the associated variation of ΔE are shown in Fig. 5. The shift of the chemical potential level to the top of the valence band at higher temperatures is accompanied by a reduction in Fermi energy E_F . In accordance with Burstein–Moss relation $E_{g\text{ term}} = E_g + 2E_F$, this leads to a reduction in optical bandgap width $E_{g\text{ opt}}$.

Thus, energies E_p and ΔE in $\text{Bi}_2\text{Te}_3\text{--Sb}_2\text{Te}_3$ crystals are not only similar in magnitude, but also have contrary trends of temperature variation: as temperature decreases, E_p increases, while ΔE goes down. This creates opportunities for their convergence at a certain temperature that depends on the ratio of Bi_2Te_3 and Sb_2Te_3 in a crystal.

For example, at $T = 300\text{ K}$, $E_p = 30\text{ meV}$ in Bi_2Te_3 (higher than $\Delta E = 20\text{ meV}$), while $E_p = 125\text{ meV}$ in

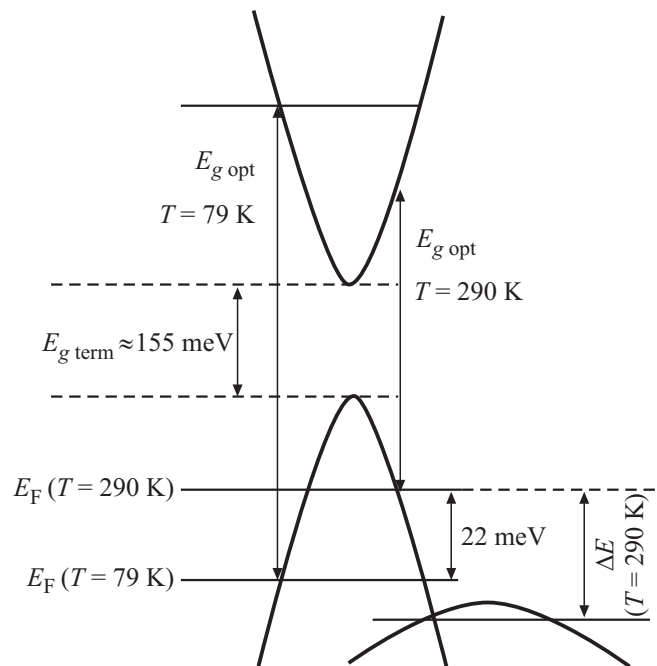


Figure 5. Band structure of the crystal containing 60 mol% Sb_2Te_3 and optical band gap values at different temperatures determined based on the results of optical studies in the infrared range [31].

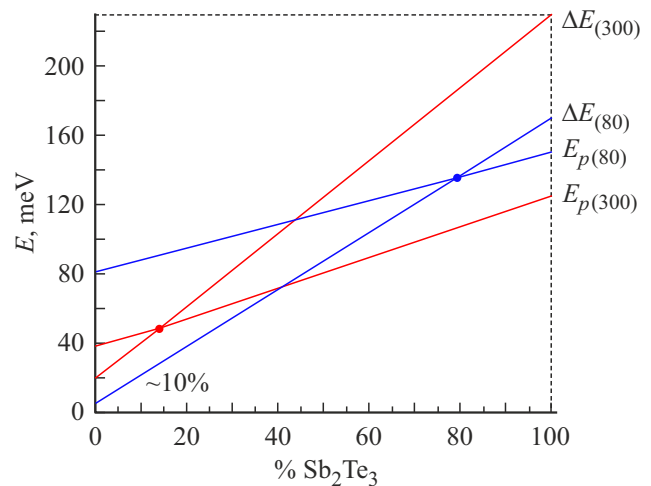


Figure 6. Dependences of plasmon energy E_p and energy ΔE of carrier transition between non-equivalent extrema of the valence band in $\text{Bi}_2\text{Te}_3\text{--Sb}_2\text{Te}_3$ crystals at temperatures of 80 and 300 K.

Sb_2Te_3 (lower than $\Delta E = 230\text{ meV}$). Therefore, plasmon energy E_p becomes equal to transition energy ΔE at $T = 300\text{ K}$ in a crystal with a certain ratio of Bi_2Te_3 and Sb_2Te_3 . It follows from Fig. 6, which presents the dependences of E_p and ΔE on the Sb_2Te_3 content of solid solution $\text{Bi}_2\text{Te}_3\text{--Sb}_2\text{Te}_3$ and the temperature, that the convergence of E_p and ΔE should be observed at $T = 300\text{ K}$ in solutions containing $\sim 10\text{--}15\text{ mol\%}$ Sb_2Te_3 and at $T = 80\text{ K}$ in crystals with $70\text{--}80\text{ mol\%}$ Sb_2Te_3 . In

view of this, the plasmon and transition energies should become equal at intermediate temperatures (80–300 K) in compositions with 10–80 mol% Sb_2Te_3 .

The following should be noted regarding the resonance nature of the effect, which is seen most clearly in the dependence of magnetic susceptibility $\chi_{||}$ of the crystal with 70 mol% Sb_2Te_3 in Fig. 1, *d*. The transition of electrons from the heavy hole subband to the light hole subband is specific in that it reduces the density of light carriers, which specify the plasma frequency and, consequently, the plasmon energy, instead of enhancing it (as in the case of thermal impurity ionization or the transition to intrinsic conductivity). A strong plasmon–electron coupling emerges as a result. Indeed, the process of generation is dominant when the plasmon energy exceeds the transition energy. Plasmons then transfer electrons into the light hole subband, and the density of light holes, which specifies the frequency of plasma oscillations, and, consequently, E_p decrease as a result. The plasmon energy becomes even closer to transition energy ΔE . At the same time, owing to filling of the hole pocket with electrons, transition energy ΔE increases, since the chemical potential level shifts to the top of the valence band. Thus, ΔE also becomes closer to the plasmon energy. Therefore, plasmon and transition energies approach each other, inducing a resonance enhancement of their interaction.

A similar effect is observed in the opposite case when the plasmon energy is lower than the transition energy and the process of recombination of electrons from the light hole subband to the heavy hole subband via an additional channel related to plasmon excitation is dominant. Since the plasmon energy is close to the transition energy, the probability of plasmon recombination is high. The density of light holes grows as a result, thus inducing an increase in the plasmon energy, which becomes closer to transition energy ΔE . In contrast, the value of ΔE decreases, since the chemical potential level shifts deeper into the valence band. Therefore, the convergence of the plasmon energy and the energy of carrier transition between extrema of the valence band in Bi_2Te_3 – Sb_2Te_3 crystals is a self-regulating resonance process.

4. Conclusion

We note in conclusion that a significant contribution of free carriers to the net magnetic susceptibility of Bi_2Te_3 – Sb_2Te_3 crystals makes it possible to probe the state of their electron system by examining the $\chi(T)$ dependences. The specific valence band structure of the studied materials enables the convergence of plasmon energy E_p and energy ΔE of electron transition from the heavy hole subband to the chemical potential level, thus intensifying the electron–plasmon interaction and inducing a strong coupling between electrons and plasmons. This sets the electron–plasmon interaction in Bi_2Te_3 – Sb_2Te_3 crystals apart from the corresponding interaction in, e.g., bismuth doped with an acceptor tin impurity [32]. The convergence

of the plasmon energy and the energy of transition from the valence band to the conduction band in bismuth doped with tin induces an increase in the density of free carriers and the plasmon energy, and the energies in electron and plasmon spectra diverge as a result.

The presence of a strong electron–plasmon coupling in Bi_2Te_3 – Sb_2Te_3 crystals, which is induced by the convergence of resonance frequencies in electron and plasmon spectra, enables the emergence of an electron system state that was predicted theoretically in [33] and is referred to as a „plasmaron“ (a bound state of a plasmon and an electron).

Funding

This study was supported financially by the Government of Zabaykalsky Krai and grant No. 22-22-20055 from the Russian Science Foundation (<https://rscf.ru/project/22-22-20055/>).

Conflict of interest

The authors declare that they have no conflict of interest.

References

- [1] B.M. Gol'tsman, V.A. Kudinov, I.A. Smirnov. *Poluprovodnikovye termoelektricheskie materialy na osnove V_2Te_3* (M., Nauka, 1972) (in Russian).
- [2] A.N. Veis, L.N. Lukyanova, O.A. Usov. *Semiconductors*, **56** (3), 230 (2022).
- [3] A.A. Kudryashov. Extended Abstract of Candidate's Dissertation (M., Mosk. Gos. Univ., 2016) (in Russian).
- [4] Y.L. Chen, J.G. Analytis, J.-H. Chu, Z.K. Liu, S.-K. Mo, X.L. Qi, H.J. Zhang, D.H. Lu, X. Dai, Z. Fang, S.C. Zhang, I.R. Fisher, Z. Hussain, Z.-X. Shen. *Science*, **325**, 178 (2009).
- [5] V.A. Kul'bachinskii, H. Ozaki, Y. Miyahara, K. Funagai. *J. Exp. Theor. Phys.*, **97**, 1212 (2003)
- [6] B. Rönnlund, O. Beckman, H. Levy. *J. Phys. Chem. Solids*, **26**, 1281 (1965).
- [7] L.D. Ivanova, Yu.V. Granatkina. *Inorg. Mater.*, **36** (7), 672 (2000).
- [8] A.A. Kudryashov, V.G. Kytin, R.A. Lunin, V.A. Kulbachinskii, A. Banerjee. *Semiconductors*, **50** (7), 869 (2016).
- [9] S.A. Nemov, Yu.V. Ulashkevich, A.A. Rulimov, A.E. Demchenko, A.A. Allahkhah, I.V. Sveshnikov, M. Dzhafarov. *Semiconductors*, **53** (5), 603 (2019).
- [10] M.K. Zhitinskaya, S.A. Nemov, T.E. Svechnikova, P. Reinshaus, E. Müller. *Semiconductors*, **34** (12), 1363 (2000).
- [11] N.P. Stepanov, V.Yu. Nalivkin, A.K. Gil'fanov, A.A. Kalashnikov, E.N. Trubitsyna. *Fiz. Tekh. Poluprovodn.*, **55** (12), 1162 (2021) (in Russian).
- [12] A. Van Itterbeek, N. Van Deynse, C. Herinckx. *Physica*, **32**, 2123 (1966).
- [13] R. Mansfield. *Proc. Phys. Soc.*, **74**, 599 (1960).
- [14] O. Busch, E. Mooser. *Helv. Phys. Acta*, **26**, 611 (1953).
- [15] N.P. Stepanov, V.Yu. Nalivkin. *Russ. Phys. J.*, **59**, 84 (2016).
- [16] M. Matyas. *Czech. J. Phys.*, **8**, 309 (1958).
- [17] M.P. Zayachkovskii, D.M. Bercha, I.F. Zayachkovskaya. *Ukr. Fiz. Zh.*, **23**, 1119 (1978) (in Russian).

- [18] A.A. Andreev, V.N. Rodionov. *Fiz. Tekh. Poluprovodn.*, **1**, 183 (1967) (in Russian).
- [19] K. Shogenji, T. Sato. *J. Phys. Soc. Jpn.*, **17**, 727 (1962).
- [20] P.M. Platzman, P.A. Wolff. *Waves and Interactions in Solid State Plasmas* (Academic, 1973).
- [21] V.B. Gildenburg, V.A. Kostin, I.A. Pavlichenko. *Phys. Plasmas*, **18** (9), 2101 (2011).
- [22] D.J. Bergman, M.I. Stockman. *Phys. Rev. Lett.*, **90** (2), 7402 (2003).
- [23] R.Charbonneau, N. Lahoud, G. Mattiuse, P. Berini. *Opt. Express*, **13** (17), 977 (2005).
- [24] A.S. Zlenko, V.M. Mashinsky, L.D. Iskhakova, S.L. Semjonov, V.V. Koltashev, N.M. Karatun, E.M. Dianov. *Opt. Express*, **20** (21), 23186 (2012).
- [25] V. M. Muravev, P. A. Gusikhin, I. V. Andreev, I. V. Kukushkin. *Phys. Rev. Lett.*, **114**, 106805 (2015).
- [26] D. Pines. *Elementary Excitations In Solids* (Basic Books, 1963).
- [27] P.A. Wolff. *Phys. Rev. Lett.*, **24**, 266 (1970).
- [28] P. Tussing, W. Rosental, A. Hang. *Phys. Status Solidi B*, **52** (2), 451 (1972).
- [29] A. Elci. *Phys. Rev. B*, **16**, 5443 (1977).
- [30] R. Sehr, L.R. Testardi. *J. Phys. Chem. Solids*, **23**, 1219 (1962).
- [31] N.P. Stepanov, A.A. Kalashnikov, O.N. Uryupin. *Semiconductors*, **55** (7), 637 (2021).
- [32] N.P. Stepanov, V.M. Grabov. *Semiconductors*, **36** (9), 971 (2002).
- [33] A.M. Dyugaev. *JETP Lett.*, **55** (5), 269 (1992).